Experimental UAV Flights to Collect Data Within Cumulus Clouds

Gautier Hattenberger, Titouan Verdu, Nicolas Maury, Pierre Narvor, Rafael Bailon-Ruiz, Grégoire Cayez, Fleur Couvreux, Gregory Roberts, Simon Lacroix

Experimental UAV flights to collect data within cumulus clouds

Gautier Hattenberger[1], Titouan Verdu[1,3], Nicolas Maury[2], Pierre Narvor[3], Raphael Bailon-Ruiz[3], Grégoire Cayez[2], Fleur Couvreux[2], Gregory C. Roberts[2,4], and Simon Lacroix[3]

[1]École Nationale de l'Aviation Civile, Université de Toulouse, Toulouse, France
[2]Centre National de Recherches Météorologiques, Université de Toulouse, Météo-France, CNRS, Toulouse, France
[3]Laboratoire d'Analyse et d'Architecture des Systèmes, Université de Toulouse, CNRS, Toulouse, France
[4]Scripps Institution of Oceanography, University of California San Diego, La Jolla, USA

Corresponding author: Gautier Hattenberger (email: gautier.hattenberger@enac.fr).

The NEPHELAE project to develop the UAV observing system used for this study was supported by Agence Nationale de la Recherche (Project-ANR-17-CE01-0003), Aerospace Valley and Météo-France.

ABSTRACT This article presents the deployment of micro UAVs to study the evolution of cumulus clouds. The dynamic nature of the environment, the difficult weather conditions, the long distances, and the limited flight performances of micro UAV systems make such missions quite challenging. After describing the missions constraints and objectives, the system's main component is depicted: it is the definition of adaptive flight patterns that allow the UAVs to track the areas of interest in the clouds autonomously, using real-time sensor readings. The system architecture is then presented, considering the information feedback and decision process made by the operators and scientists on the ground and the necessary flight autonomy of the UAVs. The complete system has been deployed during an international meteorological campaign on Barbados island, and extended with extra test flights afterward. Details of the operational organization and the achieved flights are reported. The lessons learned during the field campaign revealed the strength and weaknesses of the proposed system and possible improvements are discussed. The collected data has contributed to a better understanding of cloud evolution, demonstrating that a tight coupling of the sensors and the flight control system is a crucial point for extending the performances of UAV systems in atmospheric science.

INDEX TERMS Atmospheric science, autonomous aerial vehicles, trajectory, UAV

I. Introduction

The evolution of cumulus clouds is still not fully understood by atmospheric scientists [1], whereas their radiative effect has a strong impact on atmospheric numerical simulations. It is therefore important to have good models of their life cycle, which must be validated by experimental data [2], [3].

The classic means to gather data for the development and validation of atmospheric models are either remote sensors, on-ground or onboard satellites, or in-situ sensors onboard planes or ballons [4]. These acquisition systems do not provide enough data when it comes to sampling highly dynamic phenomena such as cumulus clouds, for which scientists need dense measurements of a series of parameters *within* clouds, the most important being pressure, temperture, humidity, liquid water content, and aerosol concentration. Heavy piloted aircraft can gather such measurements, but along trajectories limited to transects through the cloud, and they can hardly sample the same cloud twice, especially when it spans less than a few hundred meters. Lighter aircraft such as motor gliders of sailplanes are more flexible (see e.g. [5]–[7], but only a single aircraft at a time can be used for safety reasons.

UAVs offer better possibilities to fly sensors within clouds or plumes, e.g. [8]–[10], but the gathered data with single systems remain too sparse to observe a dynamic 3D phenomenon. The NEPHELAE project[1] is motivated by the need to collect dense data within cumulus clouds. Its goal is to deploy a fleet of UAVs with the appropriate sensing

[1]NEPHELAE gathers Météo France (atmosphere scientists, in charge of onboard sensor development and cloud modeling research), LAAS-CNRS (roboticists, in charge of developing cloud mapping and exploration strategies), and ENAC (experts in UAV science, responsible of the UAV structure development and flight control). NEPHELAE is the Greek name for nymphs of cloud and rain.

and decisional capacities to follow the evolution of a cloud during its complete lifespan. From the robotics point of view, exploring a cloud is different from exploring a 3D geometric environment: not only the whole environment is dynamic, but the sensors that provide measures on the environment have no "look-ahead", their data being point-wise atmospheric measures at the UAV location. The NEPHELAE system is a mix of autonomous drones adapting in real-time their trajectories based on the onboard sensor measurements, supported by a ground-based cloud cartography system that helps the scientists to take decisions and efficiently operate the fleet.

This article is an extension of previous publications [11], [12]. In addition to a synthetic presentation of the whole NEPHELAE system, its main contributions are the evaluation of a field campaign during which trade wind cumuli have been sampled, and the implementation and testing of a mechanism to automatically recover tracking failures, that greatly improves the robustness of the system. After introducing some related work, the paper defines the cumulus exploration problem and the choices that have been made to tackle it. The core element of the approach is the application of adaptative flight patterns. A specific pattern dedicated to the exploration of cloud borders, that has been particularly experimented, is depicted. Next, we present the implementation and integration of the complete system, deployed along the EUREC^{4}A campaign [13] in January and February 2020. Finally, the experiments are presented in detail, including the operational organization, an analysis of the achieved flights, the evaluation of the deployment of the proposed solution, the obtained results and the lessons learned.

II. Related work

The problem of sampling a cumulus cloud with UAVs falls in the more general category of dynamic phenomenon tracking, which has been addressed in various application contexts in the robotics community. We briefly review here some contributions on sampling atmospheric phenomena, focusing on the ones that lead to actual flights.

The CLOUD-MAP project was a NSF-founded project led by the Oklahoma State University [14], which goal was to characterize the Earth's lower atmospheric boundary layer. Several type of UAVs were involved, from light multi-rotors to 2-meter wing span planes. Most of the project publications pertain to the atmospheric sciences, but some directly concern the flight strategies, such as flocking for a fleet of drones [15], [16] – which to our knowledge has not been applied to real flights. In [17] the discussion about the concepts of operation depicts a basic flight strategy composed of vertical profiles and straight lines, without real-time information transmission from the embedded sensors to the ground operators and researchers.

The IRISS team at Colorado University [18] is developing UAVs for the support of atmospheric research. Their drones have been used in various projects [19], [20], including the EUREC^{4}A campaign [21]. The developed UAVs are particularly suited for field operations in harsh conditions, with a modular and robust design. The sampling trajectories usually consist in vertical profiles and geometric horizontal surveys, without online adaptation – this approach has been extended to cloud seeding operations [22]. Such pre-defined sampling strategies are the most used when exploiting UAVs for atmospheric research, and suffice to provide relevant data, e.g. to enhance weather predictions [23].

In [24], [25], UAVs are used for the sampling of volcano plumes. In [24], the planes are remotely piloted with First Person View (FPV) video feedback for the tracking phase, while the rest of the flight is based on predefined waypoints-based navigation. In [25], the same authors present a first strategy to optimize the trajectories, however with approximately equivalent efficiency characteristics to conventionally planned missions. The algorithm proposed in [26] tracks the plume on the basis of the CO_2 gradient, but is only evaluated in simulation.

Dynamic tracking of clouds and wind fields is also used in several work on path planing using soaring and thermals to enhance the flight time of UAVs. A well known open-source algorithm is implemented in the ArduPilot system [27]. This solution is based on a Kalman filter estimating the center of a thermal, the trajectory itself being a circle moving according to this estimated center. Other solutions are based on a reactive control using the computation of total energy variations [28], [29]. Mapping can also support the planning of optimal trajectories, instead of only limiting the estimation to the local updraft. Pioneer work in the area was carried on at the University of Sydney [30], [31], who introduced the use of Gaussian Process model to map the atmosphere. The same approach was proposed in [8], and [32] goes beyond Gaussian models. The AutoSOAR project has also provided very significant achievements [33]–[35]. One of the main issue in thermal soaring is to locate the initial location of the thermals in order to start the tracking. This can achieved thanks to onboard vision [36], which in turn can also allow to estimate the size and lifespan of the clouds [37].

The authors have contributed to several projects related to cloud exploration. During the VOLTIGE project [38], [39], a fleet of three UAVs have been deployed for the study of the Earth boundary layer. The main objective was to study the formation and evolution of fog events. The important aspects were the integration and qualification of low-cost embedded sensors inside small UAVs, the real-time communication between sensors and autopilot, and finally the coordination of spatially separated flight plans. It was also a first attempt to use adaptive trajectories by triggering events in the flight plan based on sensor readings. The project BACCHUS [40] was an atmospheric science campaign held in Cyprus. The trajectories were taking advantage of the vector-based definition of the flight primitives to perform complex patterns. We also made some studies on adaptive fleet control to explore cumulus clouds, resorting to the mapping of the cloud with

on-board sensors and the dynamic optimisation of the flights to maximise relevant data collection [41], but these have only been evaluated in simulation [42].

With respect to this significant body of work on atmospheric sampling with UAVs, the cloud sampling approach developed in the context of the Nephelae project is rather simple, e.g. it exploits individual reactive processes to ensure data collection and does not require synchronization between the UAVs. Nevertheless, it has proven its effectiveness in missions where the UAVs flew up to 8 km away from the ground station and were able to acquire a series of data considered of great interest by atmospheric scientists.

III. Problem description and approach

A. Task specification

The methodology to define the approach to gather data within cumulus clouds followed an iterative and interactive process between the atmospheric scientists and the experts of the UAV domain. A first important outcome is the modeling of the clouds to specify the interest zones, where the UAV measurements should be concentrated. Based on high resolution simulations of the physics of the atmosphere, the different stages of the cumulus clouds life cycle have been identified [43], as well as relations between the micro and macroscopic characteristics, such as the cloud base diameter, the height, the internal flows of air and liquid water, or the water droplets size. From all those information, the most important areas to explore have been defined. They are summarized on Figure 1:

- the cloud base (purple plane) is the root of most of the internal phenomenon that occur within the cloud. Assessing the vertical wind field, the humidity and the liquid water content (LWC, the measure of the mass of the water relatively to the dry air mass) allows to estimate the cloud forcing.
- the core of the cloud (cone at the center of the cloud), where the updraft is at its maximum intensity, is relevant to track during the cloud lifespan.
- horizontal layers at different altitudes (orange box), where synchronized measurements of vertical wind and LWC allow to compute the internal mass flow,
- the cloud border, which is the interface between the cloud and the open air, in which various exchanges occur (“entrainment mixing”). The measurements of the LWC at the cloud border is here key.

Our approach to collect data on these areas of interest is to resort to dedicate adaptive flight patterns [44]. These patterns do not suppose any model of the sampled phenomenon, they just adapt to its evolution. In our experiment campaign, our efforts were prioritised on the clouds border because of the rather small sizes of the encountered clouds. Section B describes in detail the dedicated pattern that has been used during the experiments.

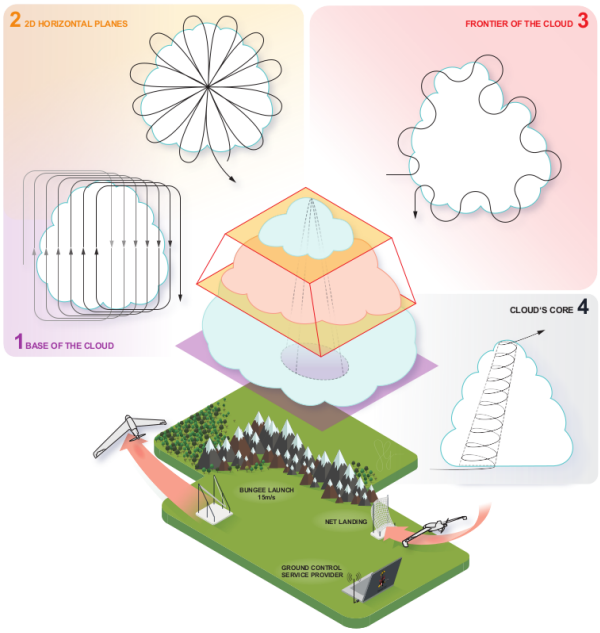

FIGURE 1: Cloud interest zones as the result of discussions with atmospheric scientists, and associated flight patterns (illustration and design by Sarah Gluschitz)

B. Problem constraints and design choices

These task specifications lead to a series of constraints for the UAVs. First, the size and shape of the cloud, as well as the length of their life cycle, impose to have an endurance of at least one hour. This is the minimum time to follow a cloud for 20 minutes under windy conditions at an altitude of at least 1000 meters above ground, including safety and operational margins. It is clear that the only viable solution with a reduced risk is to use fixed-wing planes. Rotary wing type such as multi-rotors have indeed a too limited endurance, and hybrid platform, despite their promising performances, are not mature enough, or too fragile to be used in such conditions.

The UAVs deployed are foam planes (Skywalker X6, see Figure 2) with a wingspan of 1.5m, a cruise speed around 15-20 m/s (discussed later in section 4), a maximum autonomy of one hour and a take-off weight of 2.5 kg. The Skywalker X6 can belly land on grass, but the take-off with the payload was performed using a bungee system to save energy and extend the flight duration. The project partners have operated such UAVs in previous missions [2], [3], [10], and they have proven to be robust and easy to repair (Figure 1 shows a landing in a net: such equipment have been used with this plane in previous flight campaigns, however it was not necessary this time considering the location of operation – see section A). A basic set of embedded sensors is measuring the standard atmospheric parameters of pressure, temperature and humidity (PTU). The sensing components are placed in a small metallic tube above the wing root, visible on Figure 2.

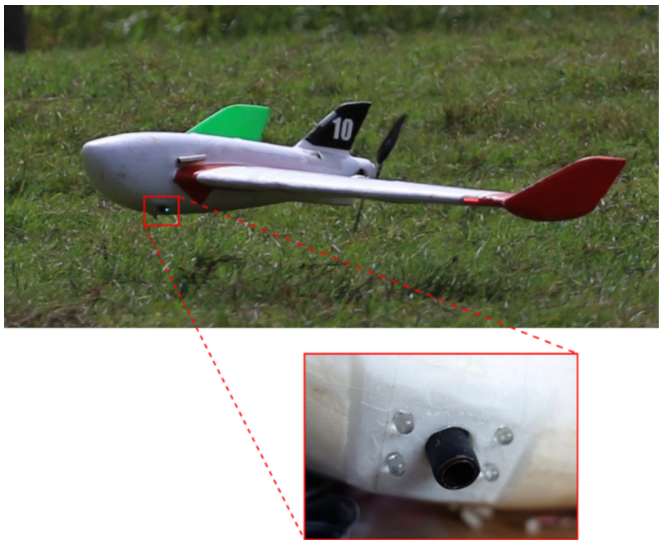

FIGURE 2: Skywalker X6 with integrated sensor for cloud detection and measurements, details in [3], [10]

The data acquisition board for the PTU sensor is a in-house design.

Considering the nature of the cumulus clouds and the interest areas, a sensor capable of detecting the cloud border without latency is needed. However, PTU data are not suited for that matter. Humidity sensors in particular do not work well above 95% of relative humidity or when there is condensation, and require significant integration time to provide accurate measures. To detect cloud borders, we resort to an optical sensor (later referred as "cloud sensor") developed by the University of Reading (UK). This sensor measures the optical extinction [10], that is the reflection of light emitted in sequence by three infrared, cyan and orange LEDs, detected by a photo-receptor. The extinction measurements are closely correlated to the LWC, a key information post-processed to assess the cloud microphysical properties. Importantly, the measurements are instantaneous, and so provide information in real time to the autopilot to determine whether the UAV is inside or outside the cloud. This information is used by the adaptive flight logic that is running on-board the autopilot hardware. This cloud sensor is placed on the side of the fuselage, oriented 45° downward to avoid perturbations from the direct sun light while protecting the device when landing, as shown on Figure 2.

Finally, the real-time communication with the ground station control is a key element for the deployment of a fleet of drones. For the current system, no direct air-to-air communication have been implemented since the planes do not require complex data sharing and processing to plan their individual trajectories and actions. The modems used are the P2400 from *Microhard*. They operate in the 2.4 GHz frequency band, with a maximum emitting power of 1 Watt and a link rate from 19.2 to 345 kbps. They have been successfully tested up to 15 km.

C. Summary of the design choices

Based on the mission requirements and constraints, the main system design choices are the following:

- A fixed-wing aircraft should be used, as it is the only type of aircraft with the required endurance and unbiased sampling of cloud microphysical properties. Considering the operational constraint to operate for a long time in a remote location in all weather conditions, a basic foam airframe, easy to repair and to modify should be preferred.
- The scientific sensors are providing scalar and local information of the environment, namely PTU and LWC provided by the cloud sensor. The cloud sensor is also used for cloud border detection, which allows the execution of the adaptive navigation patterns onboard the autopilot to efficiently sample the areas of interest around the clouds.
- The communication system should guarantee a reliable and long range connection with several planes simultaneously. A centralized network, even with a low bandwidth, is possible because the adaptive flight patterns are controlled and managed onboard by the autopilot. From sparse data received on the ground, a real-time map allows the scientists and the UAV operators to monitor the mission.

The details of the overall system architecture and its implementation are presented in section V

IV. Adaptive flight patterns

A. The flight pattern logic

The goal of the adaptive flight patterns is to efficiently collect data in the cloud areas deemed as relevant by the scientists. As mentioned in section A, in our experiments we selected the flight pattern dedicated to the cloud border, and the collected data are PTU and LWC. Additionally, this pattern is only used in 2D, at two different altitudes in the case of multiple UAVs flights.

Due to the rapid evolution of the phenomena, as well as the relatively high flight speed, on-board autonomous flight strategies are more likely to efficiently sample the different zones, especially the border of the clouds. This ensures that the pattern execution is not affected by communication latency and losses, that could lead to late reactions and hence cloud tracking failures.

Figure 3 is a synthetic view of the logic that applies to the flight patterns that rely on the crossing of the cloud borders – and in particular the one that has been been applied. During the initial phase, the aircraft is guided towards the cloud of interest. In our experiments, this is done by circling in the sky along a racetrack shape trajectory (waiting or holding pattern), until a first cloud detection occurs. After entering

the cloud for the first time, the aircraft performs maneuvers according to the current flight strategy until it reaches the border and goes out. Then a turn is commanded to re-enter the cloud and the whole process continues until reaching the end of the mission.

It as been observed during the preparation time and flight campaigns that the planes may lose track of the cloud, or more specifically, the border of the cloud. This happens when the trajectories are doing circles either completely inside or completely outside the cloud, without crossing the border for a long time. To cope with these situations, recovering strategies have been specified: when the plane makes more than a full turn without seeing the border, it will either cross in straight line if lost inside or perform circles of increasing radius around a recover point. This point is computed from the previous border detection and is taking into account the estimated horizontal wind to give an estimation of a point that is most likely inside the cloud. The evaluation of this procedure is presented in section E.

In presence of horizontal wind, the clouds drifts. Since the flight control at the navigation level is performed based on GPS coordinates, it is necessary to set a drift parameter that moves all the points related to the adaptive patterns (circle centers, segments, target and recovery points) to compensate displacement due to the wind. This parameter can be set by the operators knowing the current meteorological observations, but also from the horizontal wind estimation computed by the ground station based on the GPS track of the planes ([45], see section 3).

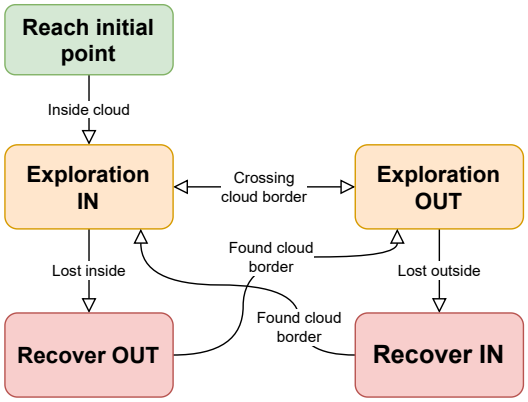

FIGURE 3: General flight pattern logic

B. Trinity flight pattern

The *Trinity* pattern is inspired by [46], where a method to estimate the boundaries of a dynamic environment with a team of robots is proposed. This strategy has been designed with the the sampling of small and medium size clouds in mind.

The logic is as follow: every time the UAV crosses the cloud border based on the sensor measurements, it records its position and heading to compute the center of the next circle that it will track, depending on the predefined turning radius. Since the direction of rotation doesn't change, the trajectory goes "backward" when the UAV is going out of the cloud and starts flying the next circle. Since the autopilot is bounding the maximum commanded bank angle, the minimum turn radius constraints is never violated. Algorithms 1, 2 and 3 describe the process in detail. Figure 4 illustrates the resulting trajectory for two different sizes of clouds.

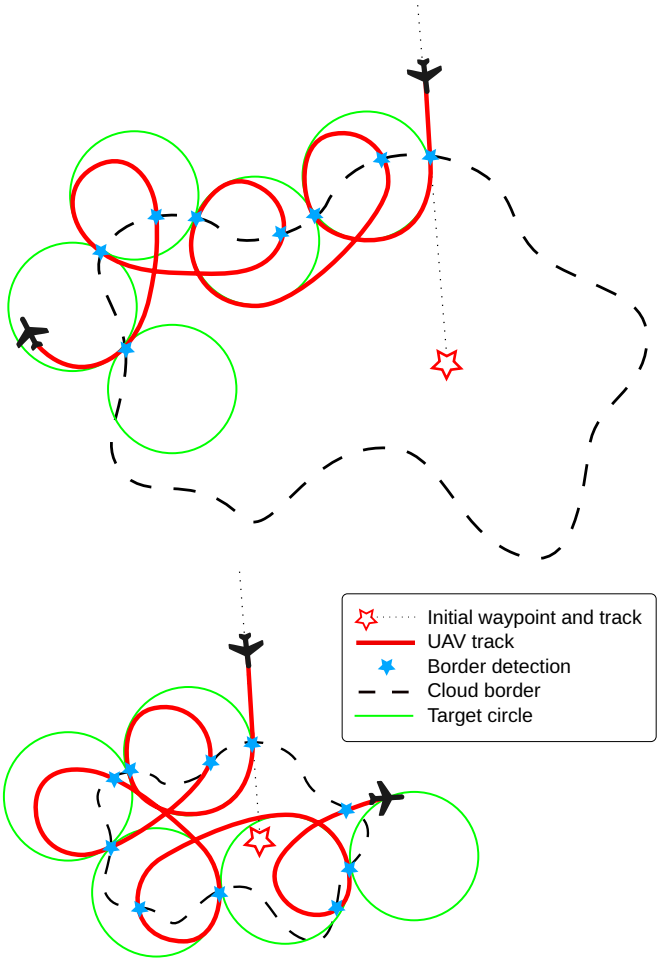

FIGURE 4: Resulting *Trinity* trajectory (in red) on a large cloud (top) and on a smaller one (bottom)

In some cases, the target circle ends up completely inside or outside the cloud, especially when the cloud evolution is very fast or its displacement relative to the ground not properly compensated. The recover procedures will try to find a new border point, either by crossing the cloud in straight line ("lost inside" case) or by flying a circle of increasing radius around a recover point. This recover point is computed based on the previous border detection. The assumption is made that this point is close enough from the border so that flying in circle around it will lead to a correct recovery. Algorithms 4 and 5 detail the recovery procedures.

Algorithm 1: *ExplorationIn* step for *Trinity* pattern

```
Global variables: init_pattern, state, initial_waypoint,
                  last_border, circle_radius, turn_direction,
                  wind_speed
Local variables : circle_center
Initialization  : init_pattern ← True
case ExplorationIn do
    if init_pattern = True then
        navigateGoto(initial_waypoint);
        if inside cloud then
            last_border ← getCurrentPosition();
            circle_center ←
              computeNextCircleCenter(circle_radius,
              turn_direction);
            init_pattern ← False;
    else
        navigateCircle(circle_center, circle_radius,
          turn_direction);
        movePointFromSpeed(circle_center,
          wind_speed);
        movePointFromSpeed(last_border, wind_speed);
        if outside cloud then
            last_border ← getCurrentPosition();
            state ← ExplorationOut;
        else if Number of turns > Max number of turns then
            state ← RecoveryOut;
```

Algorithm 2: *ExplorationOut* step for *Trinity* pattern

```
Global variables: init_pattern, state, last_border, circle_radius,
                  turn_direction
Local variables : start_step, circle_center
Initialization  : start_step ← True
case ExplorationOut do
    if start_step = True then
        circle_center ←
          computeNextCircleCenter(circle_radius,
          turn_direction);
        start_step ← False;
    navigateCircle(circle_center, circle_radius,
      turn_direction);
    movePointFromSpeed(circle_center, wind_speed);
    movePointFromSpeed(last_border, wind_speed);
    if inside cloud then
        last_border ← getCurrentPosition();
        start_step ← True;
        state ← ExplorationIn;
    else if Number of turns > Max number of turns then
        state ← RecoveryIn;
```

Algorithm 3: Compute the next circle position

```
Input: circle_radius, turn_direction
Output: circle_center
Function computeNextCircleCenter(circle_radius,
  turn_direction):
    if turn_direction = Right then
        rotation_angle ← −π/2;
    else
        rotation_angle ← π/2;
    current_position ← getCurrentPosition();
    current_direction ← getFlightDirection();
    circle_center.X ← current_position.X +
      cos(current_direction + rotation_angle) × circle_radius;
    circle_center.Y ← current_position.Y +
      sin(current_direction + rotation_angle) × circle_radius;
    return circle_center
```

C. Other flight patterns

Two other adaptive flight patterns that correspond respectively to the patterns 2 and 3 on Figure 1 were designed [44]. Based on empirical observations in simulations, both are adapted for large clouds for which the average cloud horizontal size is at least 8 to 10 times the turn radius of the UAVs. During the experimental flight campaign, clouds encountered where smaller: as a consequence, the *Trinity* pattern have been used almost exclusively. The few attempts to validate the two other patterns did not provide significant results and are not further discussed.

Other basic non adaptive flight patterns are also used during the mission, for the take-off, initial climb, cloud searching and landing phases. These flight elements mostly consist of circles and straight lines. The cloud search phase is adapted to the meteorological situation at the mission location: in our field campaign, it consists of a racetrack shape trajectory (holding pattern), centered on a geo-referenced position upwind of the ground station.

V. System integration

A. Overall architecture

The proposed overall architecture of the NEPHELAE system is represented 5. It is a centralized architecture based on the Paparazzi UAV System[2] [47], an open-source drone hardware and software project, designed with the vector-based autonomous navigation for various civil and scientific multi-UAV applications in mind. Paparazzi is well-suited to interact with external ground agents such as a dedicated mission controller [48]. The main features of the system architecture are:

- high levels goals and task allocation are set from the ground by the operators,

[2] http://paparazziuav.org

Algorithm 4: *RecoverIn* step for *Trinity* pattern when lost outside a cloud

Global variables: state, last_border, circle_radius, turn_direction, circle_radius_increment, wind_speed
Local variables : start_recover_position, init_recover
Initialization : init_recover ← True
case *RecoverIn* **do**
  if init_recover = *True* **then**
    circle_radius_offset ← 0;
    init_recover ← False;
  `navigateCircle`(last_border, circle_radius + circle_radius_offset, turn_direction);
  `movePointFromSpeed`(circle_center, wind_speed);
  `movePointFromSpeed`(last_border, wind_speed);
  if circle_radius + circle_radius_offset < *maximum radius* **then**
    circle_radius_offset ← circle_radius_offset + circle_radius_increment;
  if *inside cloud* **then**
    last_border ← `getCurrentPosition()`;
    init_recover ← True;
    state ← ExplorationIn;

Algorithm 5: *RecoverOut* step for *Trinity* pattern when lost inside a cloud

Global variables: state, last_border
Local variables : start_recover_position, init_recover
Initialization : init_recover ← True
case *RecoverIn* **do**
  if init_recover = *True* **then**
    start_recover_position ← `getCurrentPosition()`;
    init_recover ← False;
  `navigateLine`(last_border, start_recover_position);
  `movePointFromSpeed`(last_border, wind_speed);
  if *outside cloud* **then**
    last_border ← `getCurrentPosition()`;
    init_recover ← True;
    state ← ExplorationOut;

- the embedded sensors are connected to the autopilot, their data being used in real-time for cloud tracking with the adaptive patterns,
- sensor data reported (at a low frequency) to the ground is used to build a dense map of the cloud (*Cloud Adaptive Mapping System* (CAMS), see section C), to help the operator in their decisions.
- The various roles of the operators are explicitly integrated (see section B).

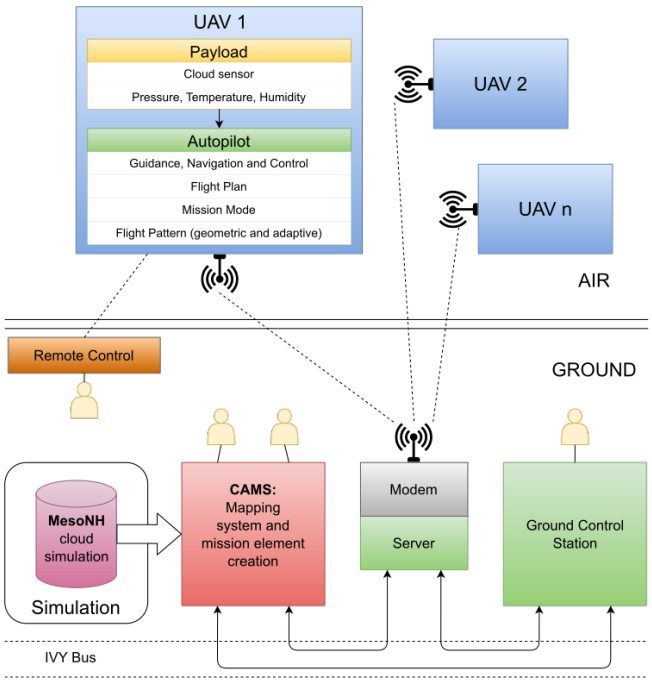

FIGURE 5: Global system architecture of the cloud adaptive mapping system

Simulations are very useful to develop and test the overall system. For this purpose, the flight dynamic is provided by the *Paparazzi* UAV system (see section B), and the meteorological scientists involved in the project provided high fidelity simulation data of the atmosphere using the MesoNH model [43], [49]. The simulated atmosphere provides all the necessary physical parameters, such as wind, temperature, humidity or LWC in a 4D spatio-temporal mesh.

B. Flight management with the Paparazzi system

With Paparazzi, the control of the UAVs is possible at different levels. In the context of this work, the most relevant ones are:

- *Flight Plans* are providing a static description language to build complex procedures, which is well suited for the take-off, waiting and landing phases. Navigation is vector-based, meaning that flight elements are described by geometric patterns rather than a list of points, making it adapted to complex and adaptive flight strategies. In addition, it can provide many layers of protections of the flight area by triggering safety procedures. This mode is also used for all the tuning flights, which concerns the aircraft themselves but also the atmospheric sensors.
- *Mission Task* control consists of a list of actions or flight patterns to be executed in a sequence. The tasks are received from the datalink system and are adapted to dynamic environment and mission management. Since

the task based control is granted by the general navigation control, it can fallback to the safety procedure at any time and restrict this mode of operation to a dedicated airspace with no risk of fly-away of a drone.

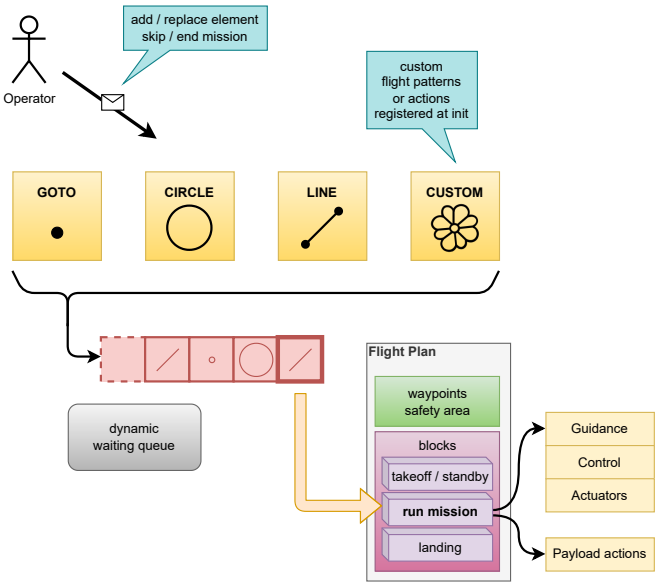

FIGURE 6: Integration of dynamic mission elements with the static flight plan description in the *Paparazzi* system. Within the static flight plan, a block called *run mission* allows to execute the mission elements from a waiting queue filled dynamic by the operator. The adaptive pattern is one of the possible custom flight pattern.

Figure 6 summarizes the interactions between the flight plan and mission task control. During the takeoff, standby and landing phases, the static flight plan is controlling the flight. When a cloud is detected, the flight plan block *run mission* is executed, which gives the control to the dynamic execution part. The flight patterns are sent from the ground as *custom* mission elements. This mode ends when the mission queue is empty, when the operator decides interrupt the mission, or when safety procedures from the flight plan are triggered.

The implementation of the flight patterns relies on *modules* that can be called either from the flight plan or as a task in the mission controller. The general navigation system is providing a set of basic flight patterns (*goto waypoints*, *fly circle*, *fly segment*, ...) that can be assembled to perform complex patterns. All the data coming from onboard sensors or other payload can be made available and used by sensor-driven sampling strategies as presented in section IV.

C. Mapping and tasks allocation

The *Cloud Adaptive Mapping System* (CAMS) is a software framework that provides a graphical user interface to create and manage flight plans adapted to cloud exploration. It can also build in real-time LWC maps from the sampled data, to help the operators make decisions about the exploration process and post-mission data analysis.

Maintaining a reliable map of the environment is of course of utmost importance for exploration tasks. Due to the sparsity of the sampling process in a dynamic 3D environment, Gaussian Process Regression (GPR) is particularly adapted for this mapping problem. CAMS builds a 4D (x, y, z, t) map using GPR on the basis of the cloud sensor data. The GPR hyperparemeters have been optimised prior to the experiments in simulation, by flying within clouds simulated by the Meso-NH atmospheric model. Data points older than a minute are not considered anymore in the GPR estimate. The map produced is compensated by the estimated wind in order to produce a map linked to the cloud moving reference frame and not the fixed Earth frame (prior work without the moving frame can be found in [41]). The map is built on a dedicated computer on ground, gathering all UAVs' measurements. In the field campaign, its only purpose was to inform the operators of the occurence of clouds along the flown trajectories, and to monitor the execution of the cloud border tracking patterns.

The second functionality of CAMS is to support the operators for creating the mission elements that are sent to the drones. This is achieved by selecting on the map the location of the starting point and the appropriate flight patterns and their parameters. Each new task has to be validated by the mission supervisor and is visible in the queue list of the graphical interface.

CAMS is also ready to work in mixed-reality scenarios, combining physical and simulated UAVs, with real or simulated cloud environments. Figure 7 shows several views of the CAMS interface during a hybrid simulation (real UAV, simulated cloud).

Finally, UAV flight trajectories and sensor data are stored in a database during mission execution for review and analysis.

VI. Flight experiments

A. The campaign location

The NEPHELAE field experiment leveraged an international flight campaign, called EUREC4A [13], [50], [51], at the beginning of 2020 on the island of Barbados. This EUREC4A campaign involves research vessels, piloted research aircraft and two other types of drones. Barbados Civil Aviation Authorities have specifically allowed UAV flights in the context of this scientific mission, as long as the drones have permit to fly from authorities of their originating country. Also, since the selected location for drones was the same for all teams, the airspace had to be shared.

Finding the right location to carry out the flights is already a challenge. The targeted clouds are trade wind cumuli, which means that the flights have to be over the sea and in the tropics. The prevailing winds speed averages 8 m/s and it is required to follow the same cloud as long as possible (the life-time of such clouds is around 20 to 30 minutes).

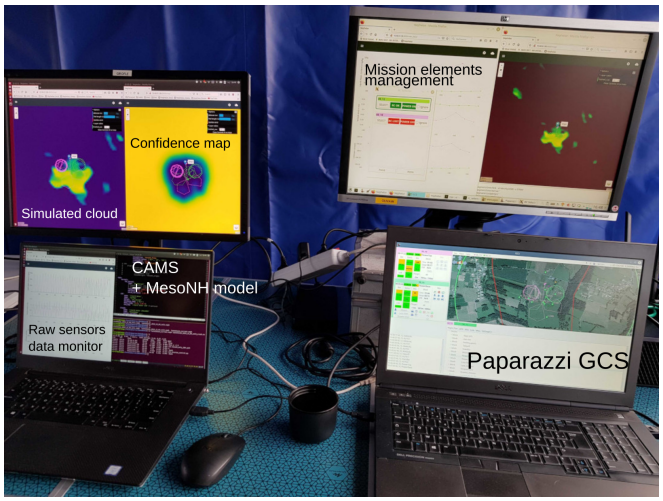

FIGURE 7: The main CAMS interface, with reference cloud and confidence of the built map (yellow background shows the unexplored area) on the top left, raw sensors data monitor (bottom left) and current list of mission elements (top right). The UAVs ground control station (GCS) is at the bottom right.

FIGURE 8: Map of Barbados Island with flight location at Morgan Lewis, Barbados Cloud Observatory (BCO) and Bridgetown Airport (BGI)

This implies that the flight area has to be large enough, with ceiling up to 2000 meters above sea level. Several places have been considered, and visited by the NEPHELAE project members prior to the mission, to assess the meteorological conditions, accessibility, local regulation, etc.

The selection of the flight location was complex as several factors had to be considered. The first constraint was to be located on the east coast as the prevailing trade wind is blowing westward from the ocean and the goal is to sample the clouds before they reach the island. The Barbados international airport (BGI) is located at the south end of the island, which means that the flight area should be located in the north to avoid conflicts with the commercial planes during their approach to BGI. Finally, for fixed-wing operations the field should be flat, far enough from populated area and void of surrounding obstacles. None of the three possible spots perfectly matched all the criteria, but a place called Morgan Lewis (see Figure 8) was the best option, with a long field well-oriented toward the sea and with few obstacles, except for hills on the side and a downward slope that made the automatic landing impossible – as a result all landings were performed by the safety pilots.

FIGURE 9: View of the temporary operation center and storage

The NEPHELAE experiments lasted 4 weeks in January and February 2020, and involved the participation of a total of 10 people (scientists, engineers, PhD students). The UAVs, ground equipment and computers, scientific sensors and batteries were sent two months in advance by ship. Containers served as the base station for operation and storage as seen in Figure 9.

B. Flights organization

As presented in section A, the flight operation strategy results from a joint problem analysis of the atmospheric scientist and the UAV experts. It is important to insist on the fact that the objectives of the NEPHELAE field experiment were driven by atmospheric science. With this in mind, and considering the overall NEPHELAE system architecture, five operator roles have been defined to carry out a complete flight operation:

- The *scientist* is monitoring the real time sensor values collected by the UAVs. When the scientist estimates that a UAV is crossing a cloud worth sampling, he/she requests to deploy a specific pattern to the *mapmaker operator*. He/she is also in charge of the analysis of the regional weather forecast and near real-time satellite images to determine if clouds are coming within the next hour.

- The *mapmaker operator* is checking the real-time cloud mapping process based on Gaussian Process Regression. Once the mapmaker receives new instructions from the scientist, he creates a new mission element with the desired parameters.
- The *UAV operator* is controlling the flights from the Ground Control Station (GCS). In particular, this operator is in charge of take-off, landing and waiting procedures, as well as the general safety of the flights.
- The *flight director* is the coordinator of the three former operators. The flight director is checking the created mission and decides if it should be accepted or rejected. He/she is also in charge of the coordination with the other teams sharing the airspace and is the point of contact for the local Air Traffic Control.
- The *safety pilot* is on the field with the UAVs remote control and is coordinating the take-off and landing phases with the UAV operator. The safety pilot can take back the control of the UAV when flying in line-of-sight and is manually piloting the take-off and landing phases.

Figure 10 shows the operation center with three dedicated displays. The flight director stands behind these three operators to have a global view of the flight operations, the safety pilot remains on the field for take-off and landing operations.

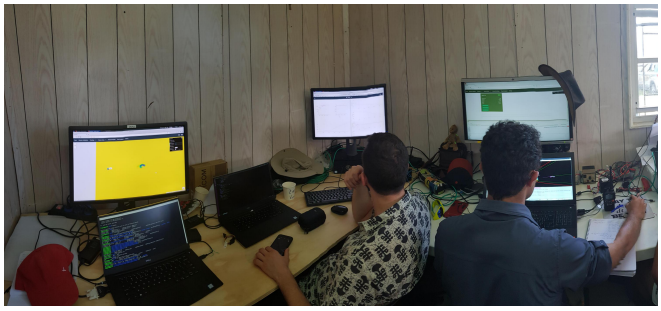

FIGURE 10: Operation center displays. From left to right: atmospheric data and mapping display for the scientists to confirm cloud detection, real-time mapping system configuration and control, and GCS for the UAV operator.

Ensuring the safety of the operations is of course an essential component of the mission. Several operators (from the NEPHELAE team but also from other teams sharing the same airspace) are involved at different levels and stages of the flights, which requires a clear and concise communication between them. One of the most critical points is the relation between the UAV operator and the safety pilot, whose task is to monitor the flight during take-off and landing from a standard remote control (RC). Considering the initial goal of the project to have up to 4 or 5 UAVs at the same time, it was not a viable option to have one qualified pilot for each drone. In addition, previous experiences have shown that the risk of mixing the RC transmitters is real and has lead to catastrophic situations.

The solution that has been selected was to use a single safety pilot with only one RC transmitter, similar to a former flight campaign in the Maldives in which three aircraft were operated simultaneously [52]. All planes were bonded to the same RC and a special software tool was developed for the UAV operator to select which plane is being controlled at a particular time. This is not without risks – if a plane is selected in the wrong mode, it might enter to a safety mode and go back home. To reduce this risk, the RC selector was also checking the status of the autopilot (autonomous flight or RC mode) to decide if the selection of a particular UAV is valid or not. A handshaking (cross validation between the RC selector and the autopilot) was in place to minimize the risk of incoherent state.

C. Flights analysis

1) Flights summary

TABLE 1: Summary table of the flights during the experimental Barbados flight campaign

Number of flights	48	22 of which achieved with two UAVs
Data recorded	45 hours	Flight time average around 53 minutes per flight
Calibration flights	23	Cloud sensor and UAV calibration, validation of the flight pattern
Measurement flights	25	Vertical profiles and cloud tracking missions
Viable scientific flights	18	Autonomous cloud tracking during more than 2 minutes. Four flights tracked clouds for more than 8 minutes, and the average tracking time is around 5 minutes.

Table 1 presents a summary of the flights during the whole campaign (more detailed satistics are provided in [51]). Each "flight" refers to a complete operation involving either one or two UAVs.

A first remark is that the number of calibration/validation flights comprised nearly half of the total number of flights. The reason is that the complete testing of the system including the sensors, adaptive sampling strategies and mapping software in real clouds could not be done before the campaign, and a number of unforeseen issues had to be addressed once operations began in the field.

Most clouds tracked during this campaign spanned between 400 and 600 meters horizontally: with a 100 meters turn radius of the UAVs, the flight pattern could effectively sample cloud borders, for an overall duration of 90 minutes. The data collecting / flight time ratio is rather poor: this was mainly limited by the allocated flight area and the wind speed, and did not prevent significant scientific analyses (section D).

Some representative flights are presented hereafter to analyse the behavior of the adaptive patterns.

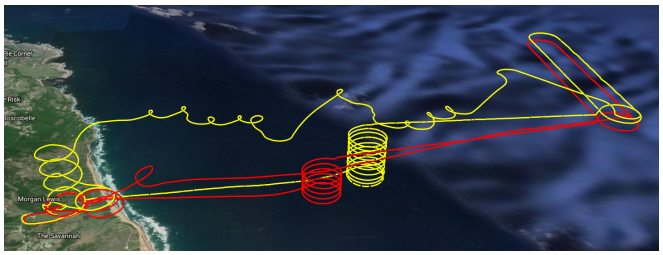

(a) The two UAVs trajectories

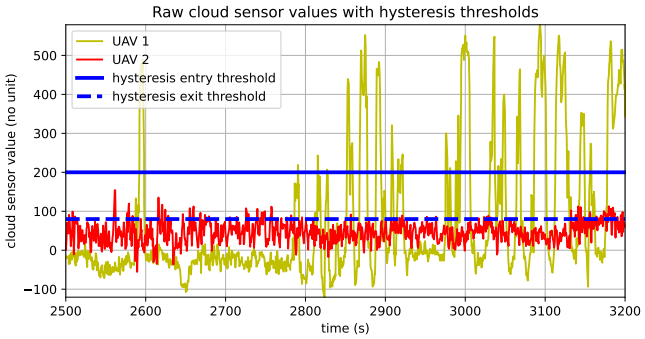

(b) Cloud sensor values

FIGURE 11: Raw cloud sensor data gathered during a flight involving two UAVs (a). Only UAV 1 (yellow) encountered and tracked a cloud. In (b), the solid blue line is the entry threshold (the UAV is declared inside the cloud when signal exceeds it) and the dashed blue line is the exit threshold (the UAV is declared out of the cloud when the signal is below it).

2) Sensor data filtering

Prior to using the cloud sensor data in real-time to apply the adaptive flight patterns, it is necessary to filter the raw signal and define detection margins.

Figure 11 shows the cloud sensor signal gathered by two UAVs, one effectively tracking a cloud, the other one never crossing a cloud. As can be seen, the sensor data have a significant variability that hinders a clear detection of the cloud borders. A low-pass filter and a median filter are applied to isolate the noise and occasional spikes from actual cloud passes. The detection of the cloud border relies on two thresholds that define a hysteresis (plain and dashed blue lines in Figure 11b): when the cloud sensor filtered value exceeds the high threshold, the UAV is declared within the cloud, if the value is lower than the low threshold, it is declared out of the cloud. The filter parameters and detection thresholds were empirically determined, based on data from calibration flights and by reading the raw values during the loitering phase while waiting for a cloud. One of the UAV was equipped with a onboard camera: post-processing analyses confirmed the detection thresholds were well correlated with cloud border crossings.

3) Flight patterns analyses

a: Two UAVs flight

The overall flight of the first case is shown in Figure 12. The red UAV detects a cloud while flying along the holding pattern, and is immediately set in tracking mode by the operator. The yellow UAV is then sent towards the the cloud.

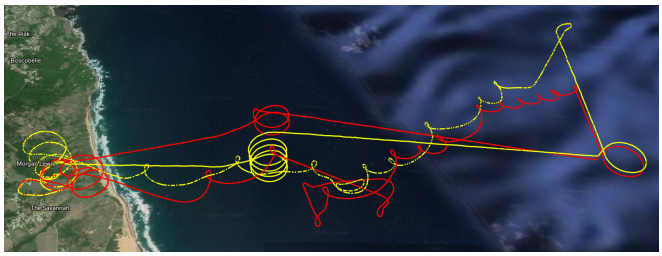

FIGURE 12: Trajectory of two UAVs during a simultaneous cloud sampling

The cloud tracking flight patterns are locally defined on the basis on the cloud border detections. In presence of horizontal wind, the resulting trajectories appear warped when plotted in the Earth global reference frame (Figure 14a). To properly analyze the flight patterns execution, the trajectory is post-processed so as to be plotted in the cloud reference frame, using the estimation of the average wind speed and direction.

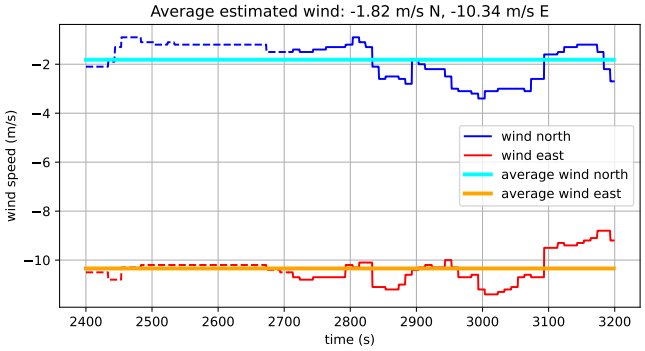

FIGURE 13: Estimated east and north wind speeds and average value during the flight of Figure 14. The dashed parts correspond to the holding patterns, while the solid lines are the estimates computed during the tracking phase.

The *Paparazzi* ground control station integrates a wind estimation algorithm based on the GPS velocity [45]. Since this algorithm only works when the UAVs are flying along a circle at constant velocity, the estimated wind is only considered when the UAVs are waiting or tracking at the target altitude. The Barbados being located within the Trade Wind Alley, the wind speed over the ocean is roughly constant in speed and direction during the time of a cloud tracking, as seen Figure 13. When the trajectory is plotted on the cloud local moving frame after correcting the drift,

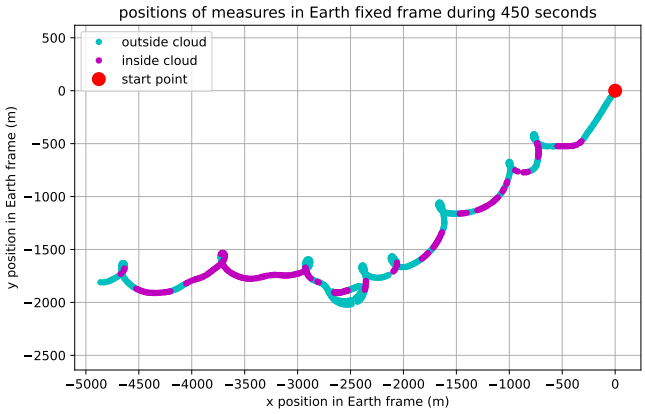

(a) Measurements in Earth frame

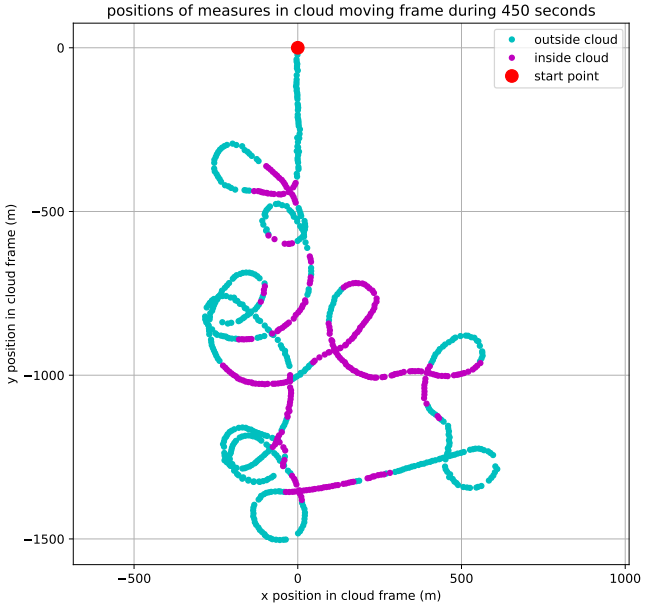

(b) Measurements in cloud moving frame

FIGURE 14: Flight trajectory of the yellow UAV of Figure 12 while tracking a cloud with the *Trinity* flight pattern, in the Earth (a) and local (b) moving reference frames. Cyan/magenta dots are measurements respectively outside/inside the cloud.

Figure 14b, the shape of the *Trinity* pattern is clearly visible. The diameter of the cloud is here around 600 meters.

Figure 15 shows the altitudes of the two UAVs as a function of time. The magenta dots correspond to the time when the UAVs are inside the cloud according to the cloud sensor. This confirms that UAV 2 (in red) starts the detection earlier than UAV 1 (in yellow). Between t = 2780s to 2950s, the two UAVs are sampling the cloud together with an altitude separation of around 80 meters. At t = 2960s, the UAV operator sends a command to UAV 2 to stop the adaptive tracking, to adjust the tracking and then resume the tracking before t = 3100s. This flight allows to observe the evolution of thermodynamic parameters at two levels, which is key to study the cloud life cycle [51]. Unfortunately, while the initial goal of the flight campaign was the deployment of a fleet of UAVs, numerous technical hurdles made that only a couple of flights could be performed with two UAVs.

b: Other flights

Figure 16 shows the trajectory of the yellow UAV of the flight Figure 11, resulting from the application of a *Trinity* pattern. This flight pattern is considered as the most robust for the small Trade Wind clouds encountered during the NEPHELAE field campaign. However, depending on the shape of the cloud, the UAV sometimes can not fulfill a complete exploration around the clouds when it fails to reenter the cloud. This occurs around the coordinates x = 400 m, y = 500 m, at the top of the Figure. Here, the operators have made the decision to stop the tracking and manually set a new target point to reenter the cloud. This interruption corresponds to the small red dots on the plot. Such cases are hard to detect using only a local perception of the cloud, but a possible solution to this problem is presented in section E.

As reported in Table 1, only 18 flights out of 48 in total are considered as viable for scientific use, i.e. when the cloud tracking lasts at least 2 minutes. Out of these 18 flights, only 2 clouds were properly tracked by two UAVs simultaneously.

Evaluating the number of turns around a cloud or the percentage of coverage of a border is difficult without an external reference. A visual inspection of the trajectories in the local cloud frame allows to evaluate that six flights achieved a full turn around the cloud border. An example of such case is shown on Figure 18, with an acceptable exploration with the *Trinity* pattern, demonstrating its efficiency in nominal conditions despite the small size of the cloud (about 200 meters).

4) Trajectory tracking and flight performances

While flying close or inside clouds, it is expected to encounter perturbations such as turbulence, downdraft or updraft. In this study, a constant altitude is required for the data collection around the cloud border.

Figure 19a shows the flight altitude of yellow UAV of the Figure 12 during the cruise and then adaptive tracking phases (right part of the figure). We can observe that during the approach phase, until 2750s, the tracking accuracy is around 5 meters. When the UAV starts the adaptive cloud tracking, after 2750s, the variations of altitude are increasing, but stay within 10 meters around the reference. An interesting point to note is that the altitude tends to increase when flying inside the cloud (magenta background areas) and to decrease when flying outside (blue background). This behavior is expected due to the nature of clouds, with updraft inside and downdraft around. The analysis of the four longest flights with two different UAVs, the average root mean square error

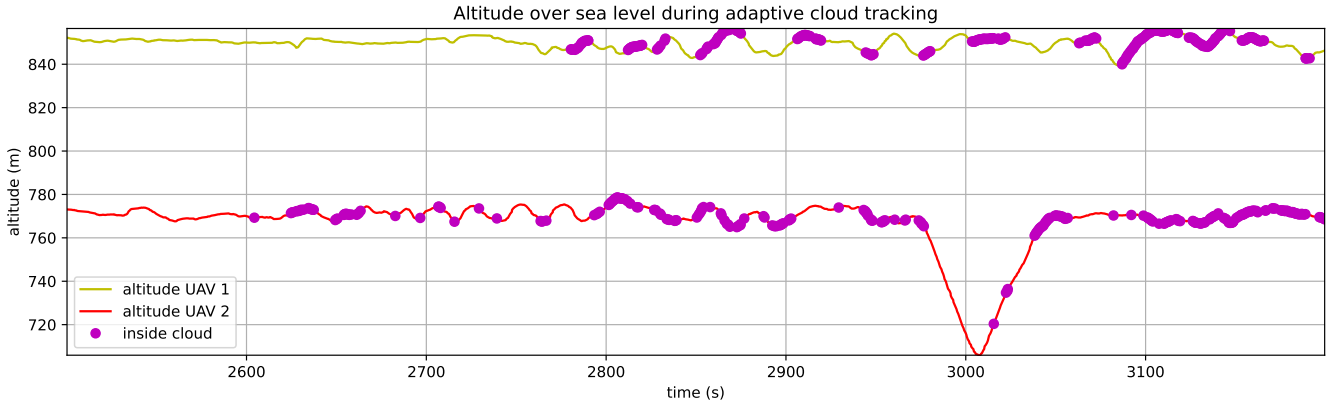

FIGURE 15: Flight altitude of the two UAVs presented Figure 12. Magenta dots correspond to the time when a UAV is inside the cloud.

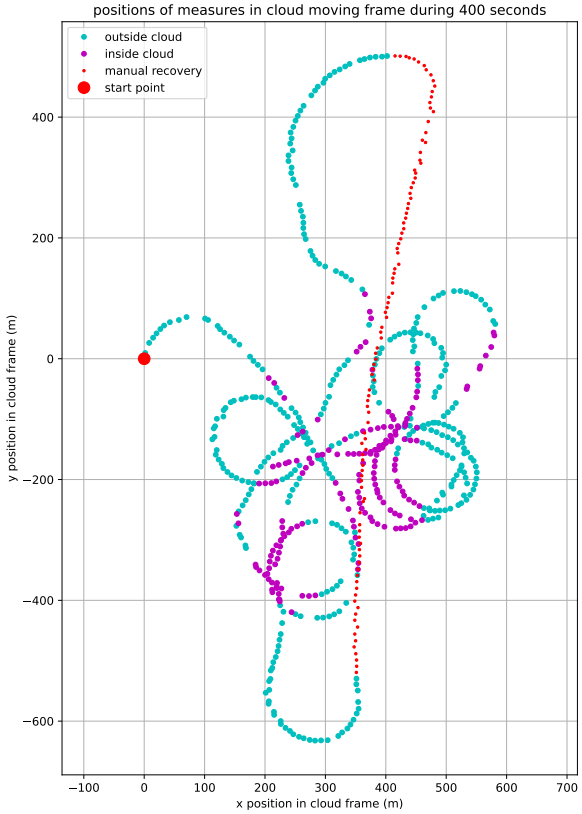

FIGURE 16: Trajectory in the local cloud frame for the red UAV of Figure 12 resulting from the execution of a *Trinity* pattern (cyan/magenta = outside/inside the cloud, red dots = adaptive tracking disabled).

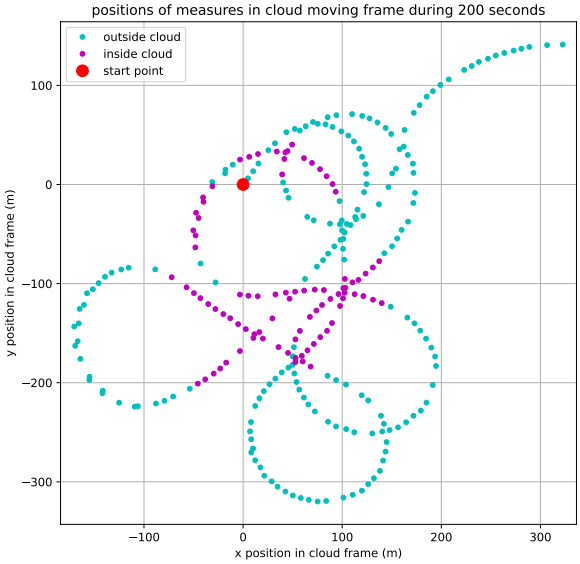

FIGURE 17

FIGURE 18: Example of trajectory in the local cloud frame resulting from the execution of a *Trinity* pattern on a small cloud (cyan/magenta = outside/inside) the cloud.

on altitude tracking is 1.43 m during the approach phase and 3.38 m during the adaptive tracking phase.

Figure 19b shows the tracking of the roll angle of the plane during the same flight phases. Until 2400s, the plane is flying headwind towards the ocean to reach the waiting area. At 2400s, it starts a turn followed by a holding pattern (race track shape) until 2700s when it is sent towards the cloud, until the adaptive tracking is effectively engaged at 2750s. The overall tracking performances are correct, even when flying at the border of the cloud. As expected, the trajectory control that is made by moving the center of a circle produces saturated roll commands (at 30°) when the UAV is outside the cloud to steer it back inside.

The oscillations on the roll angle that are observed before 2400s are explained by the heading control strategy. In order to limit the number of sensors involved in the control and state estimation, the Paparazzi system allows for fixed-wing

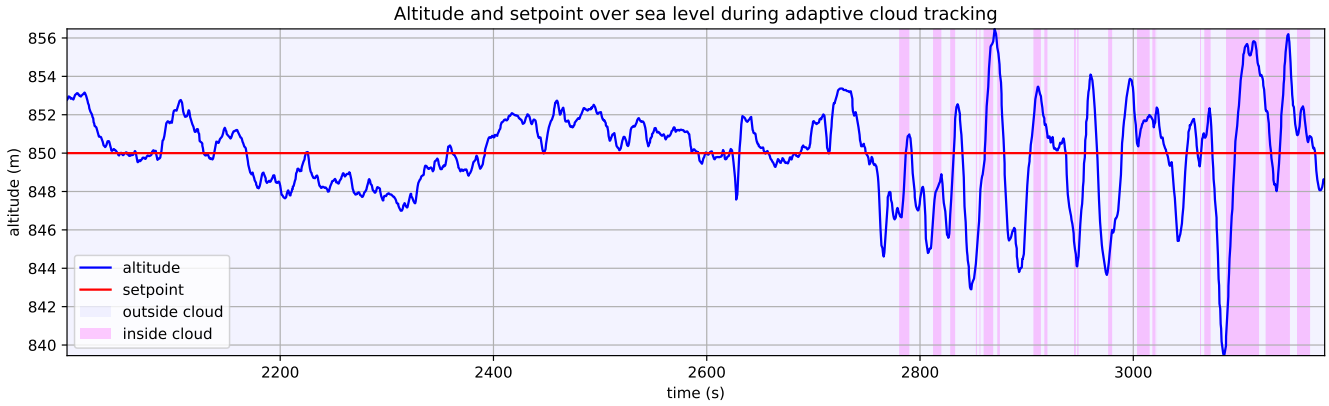

(a)

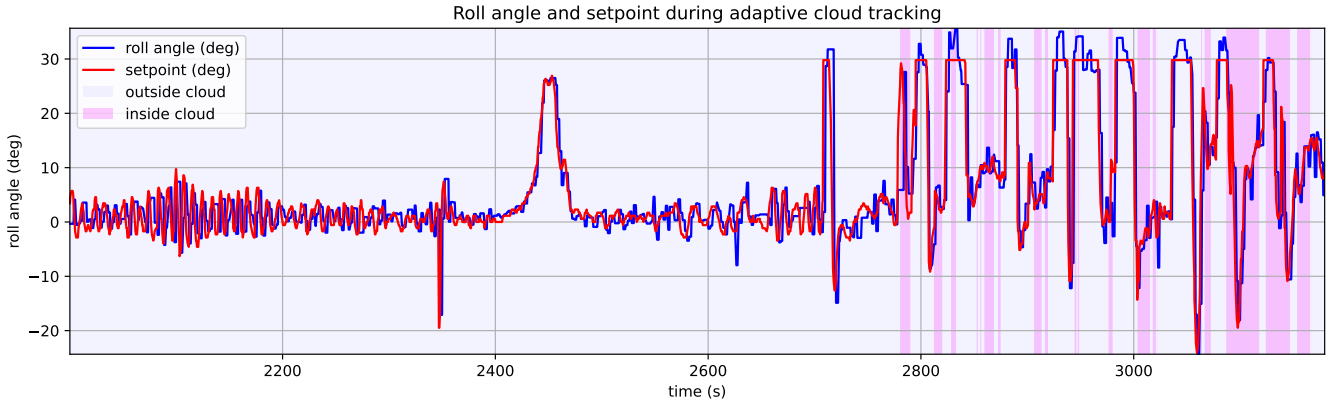

(b)

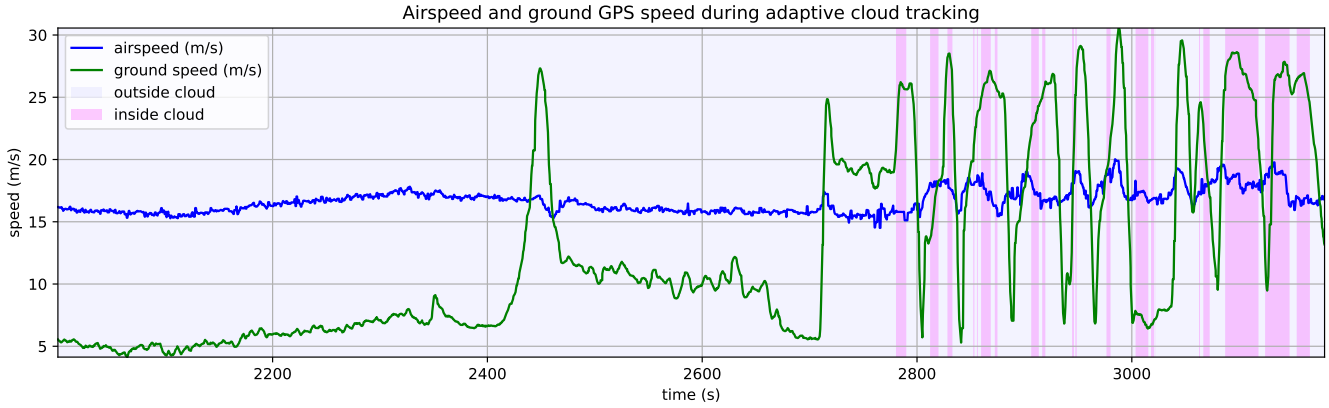

(c)

FIGURE 19: On each plots, the cruise approach phase is until t = 2750s and the adaptive cloud tracking after. The blue background corresponds to the time when the UAV is outside the cloud, while the magenta correspond to the flight inside the cloud.

aircraft to fly based on the GPS ground track rather than the real heading measured by magnetometers. When the ground speed is too low, this estimation can become unstable, and even reverse if the plane flies backward relative to the ground. Figure 19c plots the airspeed and the GPS ground speed, it shows that during the cruise phase headwind, the ground speed went down to 5 m/s, which is the minimum required to keep flying. On the other hand, the airspeed, that was constantly monitored by the UAV operator, always remained above 15 m/s, for a stall speed estimated between 10 and 12 m/s. Airspeed variations are more important during the adaptive tracking due to the cumulative effect of bank angle, altitude and wind variations.

The stall margin, that can be computed from the flight speed, the bank angle and stall speed, stays above 20% for a conservative value of 12 m/s for the stall speed in cruise flight. The minimum turn radius, which is a function of the flight speed and bank angle, varies between 40 and 70 meters for a maximum bank angle of $30°$. By default, the commanded circles have a radius of 100 meters to leave margins for control and stall protection.

During the whole flight campaign, the standard flight controller from the Paparazzi system have been used without modifications, except for an extra limitation on the maximum throttle to prevent battery voltage drop. The overall performances revealed to be acceptable for the collection of data, even at the border of the cloud where the turbulence are the strongest. All flight parameters have stayed within operational limits, although the minimum acceptable ground speed of 5 m/s have been reached several times due to the strong average wind 10 m/s and the rather low maximum airspeed of the UAVs.

D. Scientific results

The main scientific objective of the NEPHELAE project was to study the evolution of cumulus clouds and the dominant entrainment mechanism. As indicated in Table 1, 18 flights have been a priori deemed as having tracked a cloud long enough to address these atmospheric science objectives. In the end, the data acquired during 6 of these 18 flights were actually used to build diagrams of the exchange of heat and water between the cloud and the surrounding atmosphere. This has been made possible by the characterization of the thermodynamic state relating saturated/unsaturated and buoyant/non-buoyant parts of the clouds and its surroundings. The measurements done allowed to distinguish the difference between forced and actively convective clouds based on their size and thermodynamic properties. The analysis of the gathered data in this series of experiments has been published in [51], [53].

In particular, the flight in which two UAVs synchronously sampled the same cloud allowed to build thermodynamic diagrams at two different altitudes. It showed a more developed cloud with higher buoyancy and cloud water higher above cloud base, while at lower altitude, the observations converge more rapidly towards neutral buoyancy and saturated conditions as the lower part of the cloud dissipates [51].

E. Post-campaign evaluation of the tracking recovery procedure

A major concern during the mission at Barbados was that in several occasions, the UAVs lost track of the cloud after exiting it, their turning trajectory not intersecting the cloud border again. In such situations, operators had to redefine or cancel the mission by hand. A tracking recovery procedure have been added later to each of the adaptive flight pattern, as presented in section A. In order to evaluate the efficiency of this strategy, hybrid flights were conducted, with simulated clouds and real planes flying at low altitude as seen Figure 20

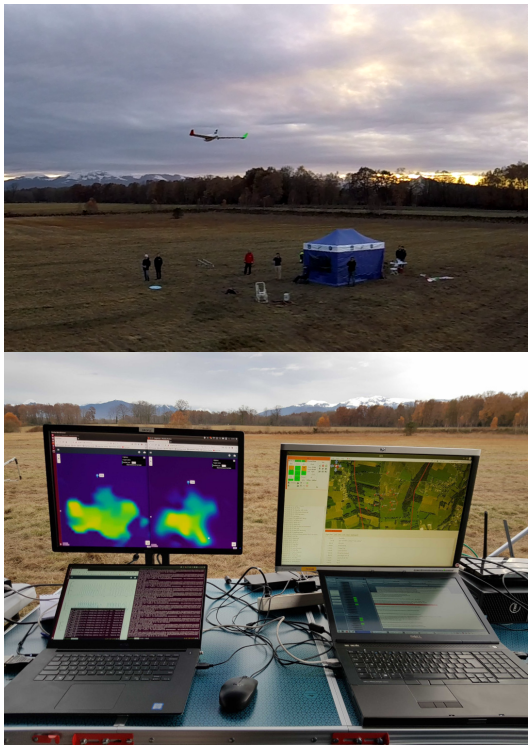

FIGURE 20: Hybrid flights with real planes and simulated cloud and sensor at Lannemezan, France

A total of 11 cloud tracking missions were done with one or two UAVs at the same time, for a total of 4 hours accumulated flight time. The simulated clouds were evolving with time, but without horizontal wind to stay within the allocated flight area.

A typical recovery sequence is presented on Figure 21. At t=-90s, the trajectory shows a spurious border detection (yellow dot) at a location far from the center of the cloud, most likely due a remaining of tiny cloud blob detached from the main part. After that, the UAV keeps turning until roughly t=-40s (one and a half full turn), before starting the recovery and heading to the recovery circle (at t=-30s). Finally, at t=0s a new border is detected, and the UAV resumes the cloud

tracking. It can be noted that the evolution of the cloud shape is quite fast during this short 4-minutes sequence.

Note that on Figure 21, the colored background represents the liquid water content (LWC) which is related to the measurements from the cloud sensor. Due to the logarithmic nature of this concentration, the shape visible on the figures are not necessarily representative of the "visible" shape of a cloud and only the highest concentrations between purple and yellow are perceptible here.

During all these 11 flights, the recovery procedure have been successfully executed. The recovery execution time was between 20 to 70 seconds, with an average time of 35 seconds. This strategy can be considered as a robust solution to the problem of cloud tracking loss.

F. Lessons learned

This experimental campaign has been an excellent opportunity to validate in the most realistic conditions the proposed approach to sample clouds with UAVs. The benefits of using robust and easily repairable aircraft have of course been clear throughout the campaign.

The first other important point is that a lot of flight time is lost in the oval trajectories, waiting for a first cloud detection. Without any additional sensor than the in-situ cloud sensor, there is no other efficient solution to detect clouds than crossing them by chance. Furthermore, encountering tiny clouds often triggered the application of a cloud tracking pattern which quickly failed, which is a waste of time and energy. Including an active cloud search capability to target specific clouds, thereby reducing the time necessary to trigger the adaptive sampling patterns, is a functionality of primary importance. A first solution could be to use a pair of ground cameras, in a wide baseline stereoscopic setup, to estimate the size location of clouds. Such a device has been developed by Meteo-France [54], but could unfortunately not be deployed on-site – and the distance at which clouds started to be tracked, up to 14 km from the shore, would have been challenging for the system. An alternate approach is to resort to an on-board camera with processing capabilities to guide the UAVs towards the clouds, without impacting the communication system, e.g. as in [36].

An other important lesson learned is that better mission management tools should be provided to the operators, in particular to the *UAV operator*. A first step would to use a high-level task planning system to automate a part of the actions currently performed by humans. The goal would be to allocate the UAVs to various tasks according to their capabilities (sensors, energy resources, ...) and to synchronize their actions, such as reaching specific locations at a given time. Both centralized and distributed solutions have been proposed for this kind of problems for UAVs [55].

From an atmosphere science perspectives, additional adaptive patterns should be defined. For instance, the presented flight patterns are all applied in a 2D plane, whereas they could be initialized with a vertical speed in order to sample more volume. An important additional pattern one would be the possibility to fly ascending and descending spirals centered on the core of the cloud. The main difficulty is that it requires a continuous signal of the cloud microphysical properties and vertical air flow, hard to estimate in such turbulent conditions.

Finally, the definition of evaluation metrics to better evaluate the efficacy of the adaptive patterns from the point of view of the data they gather would be beneficial, so as to better tune them. In the absence of ground truth, the evaluation of the achieved flight patterns can only be qualitative, and one can only state that the flight patterns could collect data that yielded atmosphere scientific analyses. It is only through more systematic simulations on a large variety of clouds that one can get better insights on the efficacy of the flight patterns, as well as on how to tune them.

VII. Conclusion

Within the NEPHELAE project, an atmospheric science driven study, a series of adaptive flight patterns and a dedicated architecture have been developed to operate multiple drones during an international field campaign to follow the evolution of clouds. Several technical and scientific problems had to be considered. They span from tackling challenges to fly beyond visual line-of-sight , in a turbulent atmosphere around cumulus cloud up to 14 km from the ground control station, to efficiently sample the atmosphere only relying on the local perception of onboard meteorological sensors. In addition to that, numerous other operational constraints had to be addressed, to deploy the whole system in a remote location and to smoothly interact with the other users of the allocated airspace.

The overall campaign was a success considering the number of flights, almost 50 performed with one or two UAVs at the same time. The applied flight strategy, as well as the control architecture, mostly developed in simulated clouds, have revealed to be efficient in an operational context. Valuable scientific data have been collected and post-processed, leading to a contribution in the field of meteorological research.

However, several remarks have to done. First, the initial goal to deploy up to 5 or 6 drones have not been achieved. This is partly explained by purely technical issues on the drones, but not only. Several limitations can be directly related to the system itself. A first critical bottleneck is the limited autonomy of the system in terms of decision and trajectory planing, which is greatly increasing the workload of the operators. A second remark that is somehow related, is the capacity of the drones to have long distance perception, which is limiting to possibility to plan long term tasks. The use of onboard and/or ground based camera system to estimate the locations of the surrounding clouds would have been decisive for this purpose. The last remark is also related to increasing the UAV's autonomy: the mapping

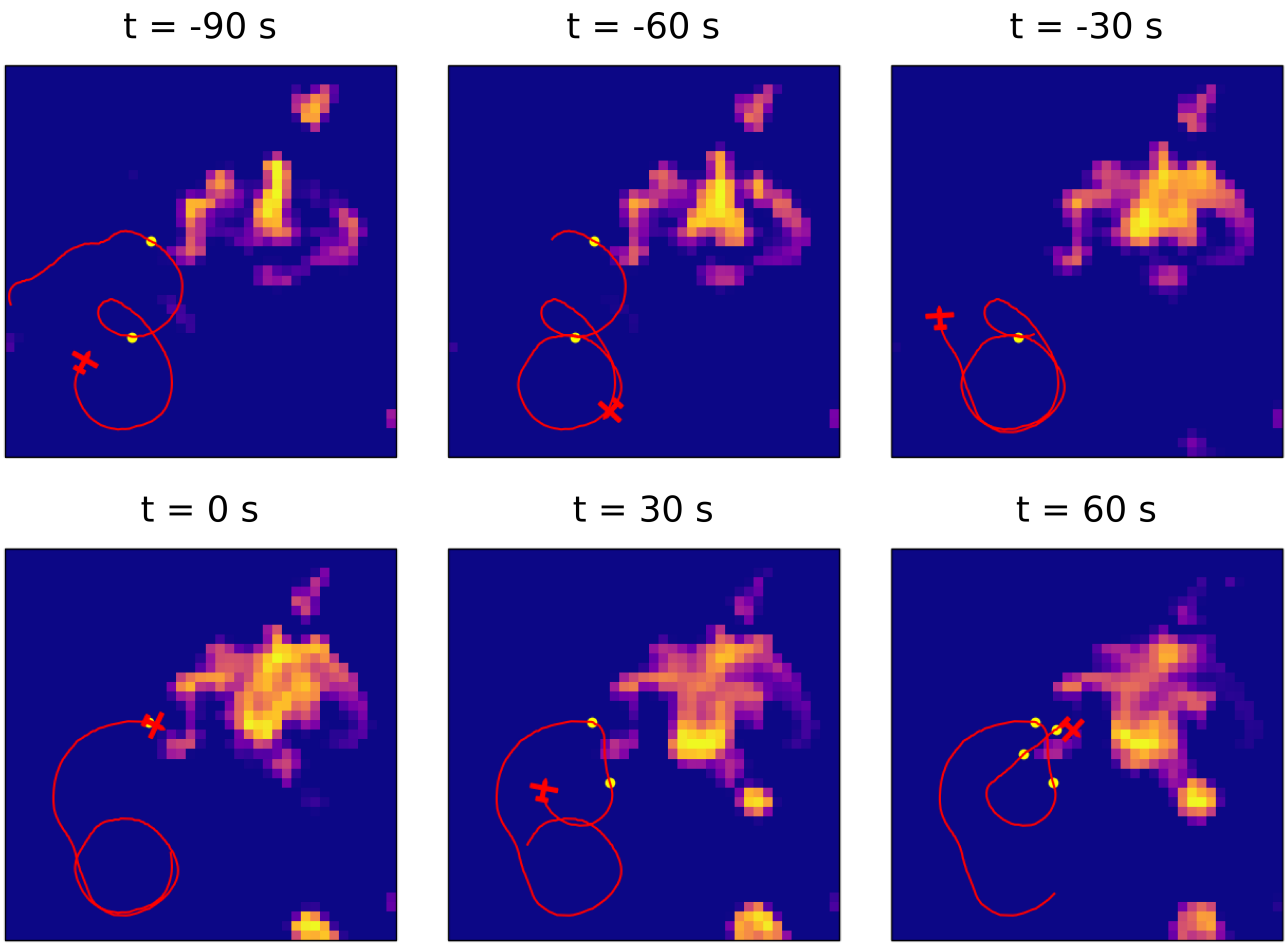

FIGURE 21: Recover sequence, with a real UAV evolving nearby a simulated cloud. The colors indicate the LWC of the simulated cloud. The UAV is turning outside the cloud between -90 and -60 seconds. It starts to head to the recover circle at -30 seconds, and finds the cloud again at t=0. Yellow dots are border detection. Note the fast evolution of the cloud with time, which is realistic.

process that was running on a dedicated ground computer was only used by the operators to trigger and monitor the execution of the cloud border tracking patterns. It hence contributed to the success of some of the flights, but it has the potential to yield more informed, hence more robust, cloud adaptative sampling tasks. Properly mapping the cloud physical parameters is key for the development of more efficient sampling schemes, and most efforts should be put on this functionality prior to studying multi-robot mission planning processes: in particular, the fusion of outer visual information and inner cloud parameters measurements would yield very informative cloud maps.

Despite the shortcomings, the proposed architecture have proved to be functional and the scientific outcomes of the project are noticeable. Flying autonomously several UAVs and tracking the same cloud for up to 20 minutes is an important achievement in the field of atmospheric science.

Author contributions

TV, SL and GH have designed the general architecture and UAV patterns for the Paparazzi autopilot. NM and FC were supervising the scientific experiments. PN and RBR conceived and developed the Cloud Adaptive Mapping System (CAMS) module. GC, TV and GH have operated the UAVs. GCR supervised the NEPHELAE project. SL and GH wrote the article.

Acknowledgment

The authors thank Murat Bronz for his contribution in operating the UAV; and Fabrice Julien and Sophian Arixi for their contributions to preparing and operating the UAVs and scientific payload.

REFERENCES

[1] W. C. de Rooy, P. Bechtold, K. Fröhlich, C. Hohenegger, H. Jonker, D. Mironov, A. Pier Siebesma, J. Teixeira, and J.-

I. Yano, "Entrainment and detrainment in cumulus convection: an overview," *Quarterly Journal of the Royal Meteorological Society*, vol. 139, no. 670, pp. 1–19, 2013. [Online]. Available: https://rmets.onlinelibrary.wiley.com/doi/abs/10.1002/qj.1959

[2] R. Calmer, G. C. Roberts, J. Preissler, K. J. Sanchez, S. Derrien, and C. O'Dowd, "Vertical wind velocity measurements using a five-hole probe with remotely piloted aircraft to study aerosol–cloud interactions," *Atmospheric Measurement Techniques*, vol. 11, no. 5, pp. 2583–2599, 2018. [Online]. Available: https://amt.copernicus.org/articles/11/2583/2018/

[3] R. Calmer, G. C. Roberts, K. J. Sanchez, J. Sciare, K. Sellegri, D. Picard, M. Vrekoussis, and M. Pikridas, "Aerosol–cloud closure study on cloud optical properties using remotely piloted aircraft measurements during a bacchus field campaign in cyprus," *Atmospheric Chemistry and Physics*, vol. 19, no. 22, pp. 13 989–14 007, 2019. [Online]. Available: https://acp.copernicus.org/articles/19/13989/2019/

[4] B. Stevens, D. H. Lenschow, G. Vali, H. Gerber, A. Bandy, B. Blomquist, J. L. Brenguier, C. S. Bretherton, F. Burnet, T. Campos, S. Chai, I. Faloona, D. Friesen, S. Haimov, K. Laursen, D. K. Lilly, S. M. Loehrer, S. P. Malinowski, B. Morley, M. D. Petters, D. C. Rogers, L. Russell, V. Savic-Jovcic, J. R. Snider, D. Straub, M. J. Szumowski, H. Takagi, D. C. Thornton, M. Tschudi, C. Twohy, M. Wetzel, and M. C. van Zanten, "Dynamics and chemistry of marine stratocumulus—dycoms-ii," *Bulletin of the American Meteorological Society*, vol. 84, no. 5, pp. 579 – 594, 2003. [Online]. Available: https://journals.ametsoc.org/view/journals/bams/84/5/bams-84-5-579.xml

[5] K. E. Haman and S. P. Malinowski, "Temperature measurements in clouds on a centimetre scale preliminary results," *Atmospheric Research*, vol. 41, no. 2, pp. 161–175, 1996. [Online]. Available: https://www.sciencedirect.com/science/article/pii/0169809596000075

[6] M. D. Maughmer, J. G. Coder, C. Wannenmacher, and W. Würz, "The design of a new racing sailplanes: A new thermal mix model and the role of transitional cfd," in *17th AIAA Aviation Technology, Integration, and Operations Conference*, 2017, p. 4091.

[7] N. Wildmann, R. Eckert, A. Dörnbrack, S. Gisinger, M. Rapp, K. Ohlmann, and A. van Niekerk, "In Situ Measurements of Wind and Turbulence by a Motor Glider in the Andes," *Journal of Atmospheric and Oceanic Technology*, vol. 38, no. 4, pp. 921 – 935, 2021. [Online]. Available: https://journals.ametsoc.org/view/journals/atot/38/4/JTECH-D-20-0137.1.xml

[8] S. Ravela, "Mapping coherent atmospheric structures with small unmanned aircraft systems," in *AIAA Infotech@ Aerospace (I@ A) Conference*, 2013, p. 4667. [Online]. Available: https://arc.aiaa.org/doi/abs/10.2514/6.2013-4667

[9] T. Egorova, N. A. Gatsonis, and M. A. Demetriou, "Estimation of gaseous plume concentration with an unmanned aerial vehicle," *Journal of Guidance, Control, and Dynamics*, vol. 39, no. 6, pp. 1314–1324, 2016. [Online]. Available: http://arc.aiaa.org/doi/10.2514/1.G001453

[10] K. J. Sanchez, G. C. Roberts, R. Calmer, K. Nicoll, E. Hashimshoni, D. Rosenfeld, J. Ovadnevaite, J. Preissler, D. Ceburnis, C. O'Dowd, and L. M. Russell, "Top-down and bottom-up aerosol–cloud closure: towards understanding sources of uncertainty in deriving cloud shortwave radiative flux," *Atmospheric Chemistry and Physics*, vol. 17, no. 16, pp. 9797–9814, 2017. [Online]. Available: https://acp.copernicus.org/articles/17/9797/2017/

[11] T. Verdu, N. Maury, P. Narvor, F. Seguin, G. Roberts, F. Couvreux, G. Cayez, M. Bronz, G. Hattenberger, and S. Lacroix, "Experimental flights of adaptive patterns for cloud exploration with UAVs," in *International Conference on Intelligent Robots and Systems, Las Vegas (USA) (Virtual)*, Oct. 2020. [Online]. Available: https://hal.archives-ouvertes.fr/hal-02614975

[12] G. Hattenberger, T. Verdu, N. Maury, P. Narvor, F. Couvreux, M. Bronz, S. Lacroix, G. Cayez, and G. C. Roberts, "Field report: Deployment of a fleet of drones for cloud exploration," *International Journal of Micro Air Vehicles*, vol. 14, p. 175682932110708, Jan. 2022. [Online]. Available: https://hal-enac.archives-ouvertes.fr/hal-03520657

[13] B. e. a. Stevens, "Eurec^{4}a," *Earth System Science Data*, vol. 13, no. 8, pp. 4067–4119, 2021. [Online]. Available: https://essd.copernicus.org/articles/13/4067/2021/

[14] NSF, "Cloud-map grant description," https://www.nsf.gov/awardsearch/showAward?AWD_ID=1539070, 2015, accessed: 2023-05-15.

[15] B. J. Wellman and J. B. Hoagg, "A discrete-time flocking algorithm for agents with sampled-data double-integrator dynamics," in *2017 American Control Conference (ACC)*, 2017, pp. 1334–1339.

[16] B. Wellman and J. Hoagg, "Sampled-data flocking with application to unmanned rotorcraft," in *2018 AIAA Guidance, Navigation, and Control Conference*, 2018. [Online]. Available: https://arc.aiaa.org/doi/abs/10.2514/6.2018-1856

[17] J. D. Jacob, P. B. Chilson, A. L. Houston, and S. W. Smith, "Considerations for atmospheric measurements with small unmanned aircraft systems," *Atmosphere*, vol. 9, no. 7, 2018. [Online]. Available: https://www.mdpi.com/2073-4433/9/7/252

[18] IRISS, "Integrated remote and in-situ sensing," https://www.colorado.edu/iriss/, 2023, accessed: 2024-05-10.

[19] M. Nicolaus, D. K. Perovich, G. Spreen, M. A. Granskog, L. von Albedyll, M. Angelopoulos, P. Anhaus, S. Arndt, H. J. Belter, V. Bessonov, G. Birnbaum, J. Brauchle, R. Calmer, E. Cardellach, B. Cheng, D. Clemens-Sewall, R. Dadic, E. Damm, G. de Boer, O. Demir, K. Dethloff, D. V. Divine, A. A. Fong, S. Fons, M. M. Frey, N. Fuchs, C. Gabarró, S. Gerland, H. F. Goessling, R. Gradinger, J. Haapala, C. Haas, J. Hamilton, H.-R. Hannula, S. Hendricks, A. Herber, C. Heuzé, M. Hoppmann, K. V. Høyland, M. Huntemann, J. K. Hutchings, B. Hwang, P. Itkin, H.-W. Jacobi, M. Jaggi, A. Jutila, L. Kaleschke, C. Katlein, N. Kolabutin, D. Krampe, S. S. Kristensen, T. Krumpen, N. Kurtz, A. Lampert, B. A. Lange, R. Lei, B. Light, F. Linhardt, G. E. Liston, B. Loose, A. R. Macfarlane, M. Mahmud, I. O. Matero, S. Maus, A. Morgenstern, R. Naderpour, V. Nandan, A. Niubom, M. Oggier, N. Oppelt, F. Pätzold, C. Perron, T. Petrovsky, R. Pirazzini, C. Polashenski, B. Rabe, I. A. Raphael, J. Regnery, M. Rex, R. Ricker, K. Riemann-Campe, A. Rinke, J. Rohde, E. Salganik, R. K. Scharien, M. Schiller, M. Schneebeli, M. Semmling, E. Shimanchuk, M. D. Shupe, M. M. Smith, V. Smolyanitsky, V. Sokolov, T. Stanton, J. Stroeve, L. Thielke, A. Timofeeva, R. T. Tonboe, A. Tavri, M. Tsamados, D. N. Wagner, D. Watkins, M. Webster, and M. Wendisch, "Overview of the MOSAiC expedition: Snow and sea ice," *Elementa: Science of the Anthropocene*, vol. 10, no. 1, 02 2022, 000046. [Online]. Available: https://doi.org/10.1525/elementa.2021.000046

[20] E. W. Frew, B. Argrow, S. Borenstein, S. Swenson, C. A. Hirst, H. Havenga, and A. Houston, "Field observation of tornadic supercells by multiple autonomous fixed-wing unmanned aircraft," *Journal of Field Robotics*, vol. 37, no. 6, pp. 1077–1093, 2020. [Online]. Available: https://onlinelibrary.wiley.com/doi/abs/10.1002/rob.21947

[21] G. de Boer, S. Borenstein, R. Calmer, C. Cox, M. Rhodes, C. Choate, J. Hamilton, J. Osborn, D. Lawrence, B. Argrow, , and J. Intrieri, "Measurements from the university of colorado raaven uncrewed aircraft system during atomic," *Earth System Science Data*, vol. 14, p. 19–31, 2022.

[22] C. Hirst, J. Bird, R. Burger, H. Havenga, G. Botha, D. Baumgardner, T. DeFelice, D. Axisa, and E. Frew, "An autonomous uncrewed aircraft system performing targeted atmospheric observation for cloud seeding operations," *Field Robotics*, vol. 3, pp. 687–724, 01 2023.

[23] D. D. Flagg, J. D. Doyle, T. R. Holt, D. P. Tyndall, C. M. Amerault, D. Geiszler, T. Haack, J. R. Moskaitis, J. Nachamkin, and D. P. Eleuterio, "On the impact of unmanned aerial system observations on numerical weather prediction in the coastal zone," *Monthly Weather Review*, vol. 146, no. 2, pp. 599 – 622, 2018. [Online]. Available: https://journals.ametsoc.org/view/journals/mwre/146/2/mwr-d-17-0028.1.xml

[24] B. Schellenberg, T. Richardson, M. Watson, C. Greatwood, R. Clarke, R. Thomas, K. Wood, J. Freer, H. Thomas, E. Liu, F. Salama, and G. Chigna, "Remote sensing and identification of volcanic plumes using fixed-wing uavs over volcán de fuego, guatemala," *Journal of Field Robotics*, vol. 36, no. 7, pp. 1192–1211, Oct. 2019.

[25] B. Schellenberg, T. Richardson, A. Richards, R. Clarke, and M. Watson, "On-board real-time trajectory planning for fixed wing unmanned aerial vehicles in extreme environments," *Sensors*, vol. 19, no. 19, Sep. 2019.

[26] J. Ericksen, A. Aggarwal, G. M. Fricke, and M. E. Moses, "Locus: A multi-robot loss-tolerant algorithm for surveying volcanic plumes," in *2020 Fourth IEEE International Conference on Robotic Computing (IRC)*, 2020, pp. 113–120.

[27] S. Tabor, I. Guilliard, and A. Kolobov, "Ardusoar: an open-source thermalling controller for resource-constrained autopilots," *CoRR*, vol. abs/1802.08215, 2018. [Online]. Available: http://arxiv.org/abs/1802.08215

[28] Z. Ákos, M. Nagy, S. Leven, and T. Vicsek, "Thermal soaring flight of birds and unmanned aerial vehicles," *Bioinspiration & Biomimetics*, vol. 5, no. 4, p. 045003, nov 2010. [Online]. Available: https://dx.doi.org/10.1088/1748-3182/5/4/045003

[29] K. Andersson, I. Kaminer, and K. Jones, "Autonomous soaring; flight test results of a thermal centering controller," in *AIAA Guidance, Navigation, and Control Conference*, 2012. [Online]. Available: https://arc.aiaa.org/doi/abs/10.2514/6.2010-8034

[30] N. R. J. Lawrance and S. Sukkarieh, "Autonomous exploration of a wind field with a gliding aircraft," *Journal of Guidance, Control, and Dynamics*, vol. 34, no. 3, pp. 719–733, 2011. [Online]. Available: https://doi.org/10.2514/1.52236

[31] J. J. Chung, N. R. Lawrance, and S. Sukkarieh, "Gaussian processes for informative exploration in reinforcement learning," in *2013 IEEE International Conference on Robotics and Automation*, 2013, pp. 2633–2639.

[32] S. Ravela, *Tractable Non-Gaussian Representations in Dynamic Data Driven Coherent Fluid Mapping*. Cham: Springer International Publishing, 2018, pp. 29–46. [Online]. Available: https://doi.org/10.1007/978-3-319-95504-9_2

[33] N. T. Depenbusch, J. J. Bird, and J. W. Langelaan, "The autosoar autonomous soaring aircraft, part 1: Autonomy algorithms," *Journal of Field Robotics*, vol. 35, no. 6, pp. 868–889, 2018. [Online]. Available: https://onlinelibrary.wiley.com/doi/abs/10.1002/rob.21782

[34] ——, "The autosoar autonomous soaring aircraft part 2: Hardware implementation and flight results," *Journal of Field Robotics*, vol. 35, no. 4, pp. 435–458, 2018. [Online]. Available: https://onlinelibrary.wiley.com/doi/abs/10.1002/rob.21747

[35] N. Depenbusch and J. Langelaan, "Coordinated mapping and exploration for autonomous soaring," in *Infotech@Aerospace 2011*. AIAA, 2011, p. 1436. [Online]. Available: https://arc.aiaa.org/doi/abs/10.2514/6.2011-1436

[36] M. Stolle, J. Bolting, C. Döll, and Y. Watanabe, "A vision-based flight guidance and navigation system for autonomous cross-country soaring uavs," in *2015 International Conference on Unmanned Aircraft Systems (ICUAS)*, 2015, pp. 109–117.

[37] M. Stolle, Y. Watanabe, C. Döll, and J. Bolting, "Vision-based lifespan and strength estimation of sub-cumulus thermal updrafts for autonomous soaring," in *2016 International Conference on Unmanned Aircraft Systems (ICUAS)*, 2016, pp. 162–169.

[38] G. Hattenberger, G. Cayez, and G. Roberts, "Flight tests for meteorological studies with MAV," in *IMAV 2013, International Micro Air Vehicle Conference and Flight Competition*, Toulouse, France, Sep. 2013, p. pp xxxx. [Online]. Available: https://hal-enac.archives-ouvertes.fr/hal-00936235

[39] G. Cayez, J.-P. Dralet, Y. Seity, G. Momboisse, G. Hattenberger, M. Bronz, and G. Roberts, "Observations and modelling of the boundary layer using remotely piloted aircraft," in *EGU 2014, European Geosciences Union General Assembly*, Vienne, Austria, Apr. 2014. [Online]. Available: https://hal-enac.archives-ouvertes.fr/hal-01059738

[40] G. Roberts, R. Calmer, K. Sanchez, G. Cayez, K. Nicoll, E. Hashimshoni, D. Rosenfeld, A. Ansmann, J. Sciare, J. Ovadneite, M. Bronz, G. Hattenberger, J. Preissler, J. Buehl, D. Ceburnis, and C. O'dowd, "multi-dimensional Cloud-aERosol Exploratory Study using RPAS (mCERES): Bottom-up and top-down closure of aerosol-cloud interactions," in *EGU 2016, European Geosciences Union General Assembly 2016*, ser. Geophysical Research Abstracts, vol. 18, Vienne, Austria, Apr. 2016, p. pp 6530. [Online]. Available: https://hal-enac.archives-ouvertes.fr/hal-01346244

[41] C. Reymann, A. Renzaglia, F. Lamraoui, M. Bronz, and S. Lacroix, "Adaptive sampling of cumulus clouds with a fleet of UAVs," *Autonomous robots*, vol. 42, no. 2, pp. 1–22, 2018. [Online]. Available: http://dx.doi.org/10.1007/s10514-017-9625-1

[42] R. Bailon-Ruiz, C. Reymann, S. Lacroix, G. Hattenberger, H. Garcia de Marina, and F. Lamraoui, "System simulation of a fleet of drones to probe cumulus clouds," in *International Conference on Unmanned Aircraft Systems*, Miami, United States, Jun. 2017. [Online]. Available: https://hal.archives-ouvertes.fr/hal-01522246

[43] N. Maury, G. C. Roberts, F. Couvreux, T. Verdu, P. Narvor, N. Villefranque, S. Lacroix, and G. Hattenberger, "Use of large-eddy simulations to design an adaptive sampling strategy to assess cumulus cloud heterogeneities by remotely piloted aircraft," *Atmospheric Measurement Techniques*, vol. 15, no. 2, pp. 335–352, 2022. [Online]. Available: https://amt.copernicus.org/articles/15/335/2022/

[44] T. Verdu, G. Hattenberger, and S. Lacroix, "Flight patterns for clouds exploration with a fleet of UAVs," in *2019 International Conference on Unmanned Aircraft Systems (ICUAS 2019)*, Atlanta, United States, Jul. 2019. [Online]. Available: https://hal-enac.archives-ouvertes.fr/hal-02137839

[45] S. Mayer, G. Hattenberger, P. Brisset, M. Jonassen, and J. Reuder, "A "no-flow-sensor" wind estimation algorithm for unmanned aerial systems," *International Journal of Micro Air Vehicles*, vol. 4, no. 1, pp. pp 15–30, Mar. 2012. [Online]. Available: https://hal-enac.archives-ouvertes.fr/hal-00934666

[46] D. Saldana, R. Assuncao, M. A. Hsieh, M. F. M. Campos, and V. Kumar, "Cooperative prediction of time-varying boundaries with a team of robots," in *2017 International Symposium on Multi-Robot and Multi-Agent Systems (MRS)*. IEEE, 2017, pp. 9–16. [Online]. Available: http://ieeexplore.ieee.org/document/8250925/

[47] G. Hattenberger, M. Bronz, and M. Gorraz, "Using the Paparazzi UAV System for Scientific Research," in *IMAV 2014, International Micro Air Vehicle Conference and Competition 2014*, Delft, Netherlands, Aug. 2014, pp. pp 247–252. [Online]. Available: https://hal-enac.archives-ouvertes.fr/hal-01059642

[48] P. Brisset and G. Hattenberger, "Multi-UAV control with the Paparazzi system," in *HUMOUS 2008, Conference on Humans Operating Unmanned Systems*, Brest, France, Sep. 2008. [Online]. Available: https://hal-enac.archives-ouvertes.fr/hal-00938715

[49] C. Lac, J.-P. Chaboureau, V. Masson, J.-P. Pinty, P. Tulet, J. Escobar, M. Leriche, C. Barthe, B. Aouizerats, C. Augros, P. Aumond, F. Auguste, P. Bechtold, S. Berthet, S. Bielli, F. Bosseur, O. Caumont, J.-M. Cohard, J. Colin, F. Couvreux, J. Cuxart, G. Delautier, T. Dauhut, V. Ducrocq, J.-B. Filippi, D. Gazen, O. Geoffroy, F. Gheusi, R. Honnert, J.-P. Lafore, C. Lebeaupin Brossier, Q. Libois, T. Lunet, C. Mari, T. Maric, P. Mascart, M. Mogé, G. Molinié, O. Nuissier, F. Pantillon, P. Peyrillé, J. Pergaud, E. Perraud, J. Pianezze, J.-L. Redelsperger, D. Ricard, E. Richard, S. Riette, Q. Rodier, R. Schoetter, L. Seyfried, J. Stein, K. Suhre, M. Taufour, O. Thouron, S. Turner, A. Verrelle, B. Vié, F. Visentin, V. Vionnet, and P. Wautelet, "Overview of the meso-nh model version 5.4 and its applications," *Geoscientific Model Development*, vol. 11, no. 5, pp. 1929–1969, 2018. [Online]. Available: https://gmd.copernicus.org/articles/11/1929/2018/

[50] S. Bony, B. Stevens, F. Ament, S. Bigorre, P. Chazette, S. Crewell, J. Delanoë, K. Emanuel, D. Farrell, C. Flamant, S. Gross, L. Hirsch, J. Karstensen, B. Mayer, L. Nuijens, J. H. Ruppert, I. Sandu, P. Siebesma, S. Speich, F. Szczap, J. Totems, R. Vogel, M. Wendisch, and M. Wirth, "EUREC4A: A field campaign to elucidate the couplings between clouds, convection and circulation," *Surveys in Geophysics*, vol. 38, no. 6, pp. 1529–1568, Nov 2017. [Online]. Available: https://doi.org/10.1007/s10712-017-9428-0

[51] N. Maury, G. C. Roberts, F. Couvreux, T. Verdu, P. Narvor, S. Lacroix, and G. Hattenberger, "Quantifying the mixing of trade-wind cumulus during the nephelae-eurec4a field campaign with remotely piloted aircrafts," *Quarterly Journal of the Royal Meteorological Society*, vol. 149, no. 752, 2023. [Online]. Available: https://rmets.onlinelibrary.wiley.com/doi/abs/10.1002/qj.4430

[52] V. Ramanathan, M. V. Ramana, G. Roberts, D. Kim, C. Corrigan, C. Chung, and D. Winker, "Warming trends in asia amplified by brown cloud solar absorption," *Nature*, vol. 448, no. 7153, pp. 575–578, 2007.

[53] G. C. Roberts, M. Nicolas, F. Couvreux, V. Titouan, P. Narvor, L. Simon, and G. Hattenberger, "Quantifying the temporal evolution of trade-wind clouds using observations and large eddy simulations," in *Fall Meeting 2022*. AGU, 2022.

[54] P. Crispel and G. Roberts, "All-sky photogrammetry techniques to georeference a cloud field," *Atmospheric Measurement Techniques*, vol. 11, no. 1, pp. 593–609, 2018. [Online]. Available: https://hal.archives-ouvertes.fr/hal-03065671

[55] Q. Peng, H. Wu, and R. Xue, "Review of dynamic task allocation methods for uav swarms oriented to ground targets," *Complex System Modeling and Simulation*, vol. 1, no. 3, pp. 163–175, 2021.

[Online]. Available: https://www.sciopen.com/article/10.23919/CSMS.2021.0022